Biochimica et Biophysica Acta 1808 (2011) 622–633

Contents lists available at ScienceDirect

Biochimica et Biophysica Acta

journal homepage: www.elsevier.com/locate/bbamem

The importance of bacterial membrane composition in the structure and function of aurein 2.2 and selected variants

John T.J. Cheng [a], John D. Hale [b], Melissa Elliott [b], Robert E.W. Hancock [b], Suzana K. Straus [a,*]

[a] Department of Chemistry, University of British Columbia, 2036 Main Mall, Vancouver, BC, V6T 1Z1, Canada
[b] Centre for Microbial Diseases and Immunity Research, University of British Columbia, #2259 Lower Mall Research Station, Vancouver, British Columbia, V6T 1Z3, Canada

ARTICLE INFO

Article history:
Received 16 June 2010
Received in revised form 8 October 2010
Accepted 20 November 2010
Available online 7 December 2010

Keywords:
Aurein 2.2
Aurein 2.3
Oriented circular dichroism
Solid state NMR
α-Helical structure
Membrane interaction
Membrane composition
Antimicrobial activity

ABSTRACT

For cationic antimicrobial peptides to become useful therapeutic agents, it is important to understand their mechanism of action. To obtain high resolution data, this involves studying the structure and membrane interaction of these peptides in tractable model bacterial membranes rather than directly utilizing more complex bacterial surfaces. A number of lipid mixtures have been used as bacterial mimetics, including a range of lipid headgroups, and different ratios of neutral to negatively charged headgroups. Here we examine how the structure and membrane interaction of aurein 2.2 and some of its variants depend on the choice of lipids, and how these models correlate with activity data in intact bacteria (MICs, membrane depolarization). Specifically, we investigated the structure and membrane interaction of aurein 2.2 and aurein 2.3 in 1:1 cardiolipin/1-palmitoyl-2-oleoyl-*sn*-glycero-3-phospho-(1′-*rac*-glycerol) (CL/POPG) (mol/mol), as an alternative to 1:1 1-palmitoyl-2-oleoyl-*sn*-glycero-3-phosphocholine(POPC)/POPG and a potential model for Gram positive bacteria such as *S. aureus*. The structure and membrane interaction of aurein 2.2, aurein 2.3, and five variants of aurein 2.2 were also investigated in 1:1 1-palmitoyl-2-oleoyl-*sn*-glycero-3-phosphoethanolamine (POPE)/POPG (mol/mol) lipids as a possible model for other Gram positive bacteria, such as *Bacillus cereus*. Solution circular dichroism (CD) results demonstrated that the aurein peptides adopted α-helical structure in all lipid membranes examined, but demonstrated a greater helical content in the presence of POPE/POPG membranes. Oriented CD and ^{31}P NMR results showed that the aurein peptides had similar membrane insertion profiles and headgroup disordering effects on POPC/POPG and CL/POPG bilayers, but demonstrated reduced membrane insertion and decreased headgroup disordering on mixing with POPE/POPG bilayers at low peptide concentrations. Since the aurein peptides behaved very differently in POPE/POPG membrane, minimal inhibitory concentrations (MICs) of the aurein peptides in *B. cereus* strain C737 were determined. The MIC results indicated that all aurein peptides are significantly less active against *B. cereus* than against *S. aureus* and *S. epidermidis*. Overall, the data suggest that it is important to use a relevant model for bacterial membranes to gain insight into the mode of action of a given antimicrobial peptide in specific bacteria.

1. Introduction

In recent years, cationic antimicrobial peptides (AMPs) have become of wide interest as possible alternatives to currently utilized antibiotics. In particular, direct-acting antimicrobial host-defense peptides are being investigated as they are rapid-acting, potent, and possess an unusually broad spectrum of activity. For these AMPs to truly become useful, however, much work is needed to understand their mechanisms of action and reduce the potential for unwanted toxicity, to make them more resistant to protease degradation and improve serum half-life, as well as to devise means of manufacturing them on a large scale in a consistent and cost-effective manner [1].

One approach to determining the mode of action of AMPs is to establish the nature of the interaction of the peptides with bacterial membranes. However, given that native bacterial membranes consist of many different types of lipids and protein complexes (with the added complexity in Gram negative bacteria of two cell envelope membranes), most studies have examined the mechanism of action for AMPs using model membranes. Over the years, a number of lipids have been used for such studies including 1,2-dimyristoyl-*sn*-glycero-3-phosphocholine (DMPC) (e.g., aurein 1.2 [2]), 1-palmitoyl-2-oleoyl-*sn*-glycero-3-phosphocholine (POPC) (e.g., MSI-78 and MSI-594 [3]), 1,2-diphytanoyl-*sn*-glycero-3-phosphatidylcholine (DPhPC) (e.g., alamethicin [4,5]), and other diacylphosphatidylcholine membranes (e.g., $K_2(LA)_xK_2$ [6]), as well as lipid mixtures such as DMPC/1,2-dimyristoyl-*sn*-glycero-3-phospho-(1′-*rac*-glycerol) (DMPG) (e.g., PGLa [7]), POPC/1-palmitoyl-2-oleoyl-*sn*-glycero-3-phospho-(1′-*rac*-

* Corresponding author. Tel.: +1 604 822 2537; fax: +1 604 822 2157.
E-mail address: sstraus@chem.ubc.ca (S.K. Straus).

0005-2736/$ – see front matter © 2010 Elsevier B.V. All rights reserved.
doi:10.1016/j.bbamem.2010.11.025

glycerol) (POPG) (e.g., MSI-78 and MSI-594 [3]), or 1-palmitoyl-2-oleoyl-*sn*-glycero-3-phosphoethanolamine (POPE)/POPG [8–13] to name but a few.

The choice of lipids to mimic a bacterial model membrane depends on a number of factors. These include the properties of the lipids, such as hydrophobic bilayer thickness, phase transition temperature, and miscibility. For example, DMPC and DMPG are often used to investigate the effect of AMPs on chain melting temperatures, because these lipids undergo a phase transition at close to room temperature (24 °C) [14]. The properties of lipids are also linked to the techniques used to investigate antimicrobial peptide–lipid interactions. For instance, differential scanning calorimetry (DSC) experiments are often performed using DMPC, DMPG, or a mixture of these lipids [14–16], because routine calorimeters operate in the range of 0–90 °C. DSC experiments that aim to probe whether antimicrobial peptides induce membrane curvature are often performed using, e.g., 1,2-dipalmitoleoyl-sn-glycero-3-phosphoethanolamine (DiPoPE) [14,17]. In some cases, the choice of lipids also depends on the ease with which the lipids form aligned bilayers, when placed on solid glass or polymer supports. POPC/POPG mixtures have traditionally been used for ^{31}P NMR studies in mechanically aligned bilayers because of the ease of preparing aligned samples [18]. Even so, some studies utilize other materials (e.g., naphthalene [19]) or direct rehydration (e.g., 1 μl of water per slide prior to sample stacking [20]), to help resolve alignment issues in order to improve lipid bilayer alignment. Finally, to completely describe peptide-membrane interactions, factors such as, e.g., peptide-to-lipid ratio, hydration, buffer composition[21], and the nature of the lipid phase [5] also need to be considered. Ultimately, the choice of lipids should be dictated by biological relevance: the results obtained from the biophysical studies should correlate to some extent with assays performed on live bacteria that assess the actual antimicrobial activity/mode of killing (e.g., MIC, membrane depolarization).

Given that only a small number of AMPs have been studied extensively in different membrane environments, the optimal bacterial model membrane which is at the same time robust and applicable for a range of methods remains elusive. The quest for suitable lipids requires a series of peptides for which a large number of biophysical and activity data are available. A number of studies from our laboratory have looked at the structure/activity relationships in the aurein 2 peptide family. Initial studies focused on the structure and membrane interaction of aurein 2.2 (GLFDIVKKVVGA**L**GSL-CO**NH$_2$**), aurein 2.3 (GLFDIVKKVVGA**I**GSL-CO**NH$_2$**), and an inactive analogue of aurein 2.3 (aurein 2.3-COOH) in DMPC/DMPG and POPC/POPG bacterial model membranes [22]. The three aurein peptides maintain high α-helical content in DMPC/DMPG vesicles at all peptide concentrations, but show reduced α-helical content in POPC/POPG at low peptide concentrations. We have demonstrated that these peptides significantly perturb 1:1 DMPC/DMPG (mol/mol) membranes, but are less efficient at perturbing 3:1 POPC/POPG (mol/mol) membranes. A comparison of the trends observed for these three peptides in model membranes with MIC and diSC$_3$5 assay results in live bacteria (*Staphylococcus aureus* strain C622) have suggested that a 1:1 POPC/POPG (mol/mol) mixture may be the best model membrane for studying the mechanism of action of these aurein peptides against *S. aureus*.

In addition to the three peptides mentioned above, we have investigated three related peptides that contain mutations at residue 13 (the one point of difference between aurein 2.2 and aurein 2.3), denoted L13A, L13V, and L13F, and two peptides with C-terminal truncations of 3 and 6 residues, denoted aurein 2.2-Δ3 and aurein 2.2-Δ6, respectively [23]. These peptides were chosen in order to further deduce how a conservative mutation at residue 13 or the absence/presence of C-terminal residues may have an impact on the mode of action. As the data presented therein demonstrates [23], relatively conservative substitutions at position 13 (from L to A, F, or V) did not have a considerable effect on structure, membrane interaction, and activity. Complete removal of residue 13, on the other hand, reduced the helical content of the peptides in the presence of membrane, limited the ability of the peptide to insert into membranes, and abolished the ability of the peptides to kill Gram positive bacteria such as *S. aureus* and *S. epidermidis*. The biophysical component of these studies was conducted in POPC/POPG model membranes, which was proposed to be an ideal model bacterial membrane for *S. aureus* in our previous studies [22] and in many studies of other antimicrobial peptides [24–26].

Although phosphatidylcholine/phosphatidylglycerol (PC/PG) model membranes have been used extensively over the years [2,27–35], a number of recent studies have adopted other lipids mixtures proposed to be more "relevant", including phosphatidylethanolamine (PE)/PG [8–13] and cardiolipin (CL)/PG [36,37]. Indeed, recent studies have primarily been conducted in model membranes consisting of different POPE/POPG ratios [38] (mol/mol or w/w), including 3:1 [8,9,12,13,19], 7:3 [11,17,39], and 3:2 [40], to name a few, and CL/PG. Therefore, it was important to assess whether these lipid mixtures are better model membranes than POPC/POPG for the aurein 2 peptide family. In the study reported here, we have therefore chosen to compare the structure and membrane interactions of the aurein peptides in 1:1 POPE/POPG and 1:1 CL/POPG (mol/mol) membranes. Since 1:1 CL/POPG has been deemed to be a model [41] for Gram-positive bacteria such as *S. aureus* [42], the structure and membrane interaction of aurein 2.2 and aurein 2.3 in this environment was determined using solution circular dichroism (CD) spectroscopy, oriented CD (OCD) and solid state ^{31}P NMR methods. The results are compared to the biophysical data obtained in POPC/POPG and to the MIC data and membrane depolarization data using *S. aureus* C622. Next, the structure and membrane interaction of aurein 2.2, aurein 2.3, and the five variants of aurein 2.2 described above were also investigated in 1:1 POPE/POPG (mol/mol) lipids, a possible model for other Gram positive bacteria, such as *Bacillus cereus*. The conformation of these peptides is determined using CD. Oriented CD (OCD) and solid state ^{31}P NMR studies are again used to examine the interaction between these peptides and POPE/POPG. The minimal inhibitory concentration (MIC) of each peptide against *B. cereus* strain C737 was determined in order to correlate the behavior of the aurein peptides observed in model membranes to that observed in the presence of intact bacteria. In addition, the MICs were determined against *P. aeruginosa* (PA01) and *E. coli* (UB1005), which contain ~60% and ~80% PE, respectively. Overall, these data allowed us to determine the relevant model bacterial membranes for studying the behavior of the aurein peptides in different bacteria, and to better understand how sequence modulated structure–function relationships in different model membrane environments.

2. Materials and methods

2.1. Materials

Fmoc-protected amino acids, Wang and Rink resin, 2-(1 H-benzotriazol-1-yl)-1,1,3,3-tetramethyluroniumhexafluorophosphate (HBTU) were purchased from Advanced ChemTech (Louisville, KY). *N*-hydroxybenzotiazhole (HOBt) was obtained from Novabiochem (San Diego, CA). *N,N*-dimethylformamide (DMF), dichloromethane (DCM), acetonitrile (AcN) and potassium nitrate were purchased from Fisher Chemicals (Nepean, ON). *N,N*-diisopropylethylamine (DIEA), trifluoroacetic acid (TFA), ethane dithiol (EDT), triethylsilane (TES) were obtained from Sigma-Aldrich (St. Louis, MO). Mylar plates were made by cutting Melinex Teijin films from Dupont (Wilton, Middlesbrough, UK). 1-Palmitoyl-2-oleoyl-*sn*-glycero-3-phosphocholine (POPC),1-palmitoyl-2-oleoyl-*sn*-glycero-3-phosphoethanolamine (POPE), 1-palmitoyl-2-oleoyl-*sn*-glycero-3-[phospho-*rac*-(1-glycerol)] (POPG), and bovine heart cardiolipin (CL) were purchased from Avanti Polar Lipids (Alabaster, AL) and obtained dissolved in chloroform.

2.2. Methods

2.2.1. Peptide synthesis

Aurein parent and mutant peptides were synthesized as previously described [43], using a CS Bio Co. peptide synthesizer (Menlo Park, CA) by the in situ neutralization Fmoc chemistry, using Rink or Wang resin with double-coupling, as appropriate.

2.2.2. Purification

The crude peptide product was purified by preparative RP-HPLC on a Waters 600 system (Waters Limited, Mississauga, ON) with 229 nm UV detection using a Phenomenex (Torrance, CA) C4 preparative column (20.0 μm, 2.1 cm × 25.0 cm) as previously described [22,43]. The identity of the products was verified using electrospray ionization (ESI) mass spectrometry and MALDI-TOF as previously described [22,43] and confirmed to be ≥ 99% pure. The molecular weights of the five aurein mutant peptides in this study (as well as aurein 2.3) can be found in Table 1 of reference [23].

2.2.3. Solution circular dichroism (CD) sample preparation

Solution CD samples with a constant peptide concentration of 200 uM were prepared in different peptide to lipid (P/L) molar ratios of 1:15, 1:50, and 1:100, using the 1:1 lipid mixtures of CL/POPG or POPE/POPG. Appropriate amount of lipids in chloroform were dried using a stream of nitrogen gas to remove most of the chloroform and vacuum dried overnight in a 5.0 ml round bottom flask. After adding 450.0 μl of ddH_2O and 50 ul of peptide stock solution in ddH_2O to dried lipids, the mixture was sonicated in a water bath for a minimum of 30 min (until the solution was no longer turbid) to ensure lipid vesicle formation. For all samples, corresponding background samples without peptides were prepared for spectral subtraction.

2.2.4. Mechanically oriented sample preparation

Solid state NMR samples were prepared using three different P/L molar ratios of 1:15, 1:80 and 1:120. The amount of lipids (dissolved in chloroform) was kept constant at 9.59 μmol. The lipids were dried using a stream of nitrogen gas to remove most of the chloroform and vacuum dried overnight in a 5.0 ml round bottom flask. Then, the appropriate amount of peptide was added and the mixture was redissolved in 500.0 μl of ddH_2O by sonication. The mixture was deposited in 10.0 μl portions repeatedly onto 9 Mylar plates placed in a Petri dish. Between depositions, most of ddH_2O was evaporated before the next portion was deposited onto the plate. The plated samples were then placed in a 93% relative humidity chamber and were indirectly hydrated by incubating at 37 °C for 6 days (CL/POPG) or 7 days (POPE/POPG). The humidity of the samples was verified by visual inspection. The degree of alignment was verified by solid state ^{31}P NMR. Consistent sample preparation was verified by preparing two to three samples for each lipid composition and peptide concentration. Finally, the plated samples were wrapped in a thin layer of parafilm and placed in plastic sheathing before data acquisition.

Oriented CD samples were prepared in a similar fashion as described above. The peptide amount was kept constant at 0.5 μmol and mixed with appropriate molar ratios of lipids and sonicated in 2.0 ml of ddH_2O. Each mixture was deposited in 90.0 μl portions onto 3.0 cm × 1.0 cm and 1.0 mm thick quartz slides, cleaned thoroughly with ddH_2O and ethanol prior to sample preparation. Clear layers of samples were observed on the slides after indirect hydration of the samples. Prior to CD spectral acquisition, each sample was covered with a second slide with a spacer (six layers of stacked parafilm in a rectangular 3.0 cm × 1.0 cm frame with 2.0 mm width) in between.

2.2.5. Circular dichroism

Solution and oriented CD experiments were carried out using a JASCO J-810 spectropolarimeter (Victoria, BC) at 30 °C as previously described [43]. Briefly, the spectra were obtained over a wavelength range of 190–250 nm, using continuous scanning mode with a response of 1 s with 0.5-nm steps, bandwidth of 1.5 nm, and a scan speed of 50 nm/min. The signal/noise ratio was increased by acquiring each spectrum over an average of three scans. Finally, each spectrum was corrected by subtracting the background from the sample spectrum. Solution CD samples were placed in a cell (0.1 cm in length) in 200 μL portions, while the oriented CD samples on quartz slides (as described above) were directly placed in the sample compartment. The temperature of the sample compartment was kept constant by means of a water bath. The CD experiments were repeated twice in the case of solution CD and three to four times in the case of OCD. Linear dichroism effects were tested for and found not to contribute to the signal.

2.2.6. NMR spectroscopy

Solid state ^{31}P NMR experiments on mechanically aligned lipid bilayer samples were carried out on a Bruker 500-MHz NMR spectrometer (Milton, ON) at 30 °C, operating at a phosphorus frequency of 202.40 MHz as previously reported [43]. The 90° pulse was set to 11.25 μs for all samples, and a 3 s recycle delay was used. The spectra were acquired using 2048 scans and processed with 50 Hz line-broadening.

2.2.7. MIC determination

Minimal inhibitory concentrations (MIC) for L13A, L13F, L13V, aurein 2.2-Δ3, and aurein 2.2-Δ6 were determined based on the previously described modified methodology [44]. Briefly, 18 h cultures of *B. cereus* C737 grown in Mueller Hinton (MH) medium (Difco, Oakville, ON) were diluted to ~2×10^5 CFU/ml. 90 μl of diluted culture was then dispensed into a 96-well polystyrene microtitre plate (Costar, Cambridge, MA). Separately, two-fold serial dilutions in sterile MH broth of the respective peptide were carried out at 10× final concentration before 10 μl of each dilution was transferred to the

Table 1
Amino acid sequence and minimal inhibitory concentrations (MICs) in μg/ml of the aurein peptides and gramicidin S (GMS) (control) against *B. cereus*, *P. aeruginosa*, and *E. coli* (see text for experimental details). MICs are given as the most frequently observed value obtained from repeat experiments.

Peptide	Sequence	MIC (μg/ml)		
		B. cereus C737	*P. aeruginosa* PAO1	*E. coli* UB1005
Aurein 2.2	GLFDIVKKVVGA**L**GSL	128	>128	64
Aurein 2.3	GLFDIVKKVVGA**I**GSL	128	>128	32
Aurein 2.3-COOH	GLFDIVKKVVGAIGSL-COOH	>128	>128	>128
L13A	GLFDIVKKVVGA**A**GSL	>128	>128	>128
L13F	GLFDIVKKVVGA**F**GSL	128	>128	64
L13V	GLFDIVKKVVGA**V**GSL	128	>128	64
Aurein 2.2-Δ3	GLFDIVKKVVGA**L**	64	>128	32
Aurein 2.2-Δ6	GLFDIVKKVV	>128	>128	128
GMS	L(D-)FPVOL(D-)FPVO	2	–	–

culture and grown for 18 h at 37 °C before being read. The MIC was recorded as the lowest concentration of peptide in which no visible growth could be observed. In addition, culture only and broth only wells were used. The same procedure was used for cultures of *P. aeruginosa* PA01 and *E. coli* K-12 strain UB1005.

3. Results

3.1. Secondary structure of aurein peptides

To verify that aurein peptides remained structured in the presence of different lipid membranes, solution CD experiments were performed in 1:1 CL/POPG (mol/mol) and 1:1 POPE/POPG (mol/mol) small unilamellar vesicles (SUVs).

Fig. S1 shows solution CD results of aurein 2.2, aurein 2.3 and aurein 2.3-COOH in 1:1 CL/POPG (mol/mol) and 1:1 POPE/POPG (mol/mol) SUVs. All spectra demonstrated a maximum at 195 nm and two minima at 207 nm and 222 nm, which is characteristic of α-helical structures. This demonstrates that these aurein peptides adopt an α-helical conformation, regardless of the specific membrane composition. As previously observed [43], similar intensities were found at all peptide-to-lipid molar ratios (P/L = 1:15, 1:50, and 1:100) studied, indicating that maximum binding of the peptide to the lipid vesicles occurred [2]. The solution CD spectra for the five aurein variants in 1:1 CL/POPG (mol/mol) and 1:1 POPE/POPG (mol/mol) SUVs were similar to those obtained for aurein 2.2, aurein 2.3, and aurein 2.3-COOH (Figs. S2 and S3). This indicates that all the aurein peptides predominantly adopted an α-helical structure in all lipid environments tested to date [22,23].

To determine the secondary structural content of the aurein peptides in CL/POPG and POPE/POPG SUVs, all spectra were fitted using the three different programs CDSSTR [45], CONTINLL [46], and SELCON3 [47–50]. Fig. 1 shows the percentage helical and random coil content as a function of P/L ratios for aurein 2.2, aurein 2.3, and aurein 2.3-COOH in CL/POPG (Fig. 1b) and POPE/POPG (Fig. 1c). Previous results in POPC/POPG (Fig. 1a) are reproduced here for direct comparison [22]. The results showed that the percentage of α-helical content decreased and the percentage of random coil content increased as the P/L molar ratio decreased, for all lipid compositions. At high peptide concentrations, aurein 2.2, aurein 2.3, and aurein 2.3-COOH adopted close to 100% α-helical conformation, in all cases. At lower peptide concentrations, however, differences in helical content were observed. At a 1:100 P/L ratio, the three peptides adopted ca. 64–74% helical structure in POPC/POPG, 34–54% helical structure in CL/POPG, and 60–73% helical structure in POPE/POPG. Overall, the data show that the structures of the aurein 2.2, aurein 2.3, and aurein 2.3-COOH were retained, but the structural content was dependent on the molar concentrations examined and also on lipid composition, in particular when cardiolipin was present.

Fig. 2 shows the percentage of secondary structure content as a function of P/L ratios for the five aurein variants: L13A, L13V, L13F, aurein 2.2-Δ3, and aurein 2.2-Δ6. The results again showed that the percentage of α-helical content decreased and the percentage of random coil content increased as the P/L molar ratio decreased, for all lipid compositions. At low peptide concentrations, the results suggest that the helical content is slightly higher for POPE/POPG membranes, followed by POPC/POPG, and then CL/POPG SUVs.

3.2. Membrane insertion states of aurein peptides

Understanding how the aurein peptides interact with different model bacterial membranes is crucial to elucidating the effect of membrane composition on the extent of peptide insertion into the lipid bilayers. OCD experiments were conducted to investigate the peptide insertion profiles in 1:1 CL/POPG (mol/mol) and 1:1 POPE/POPG (mol/mol) bilayers. For both OCD and ^{31}P solid state NMR (see

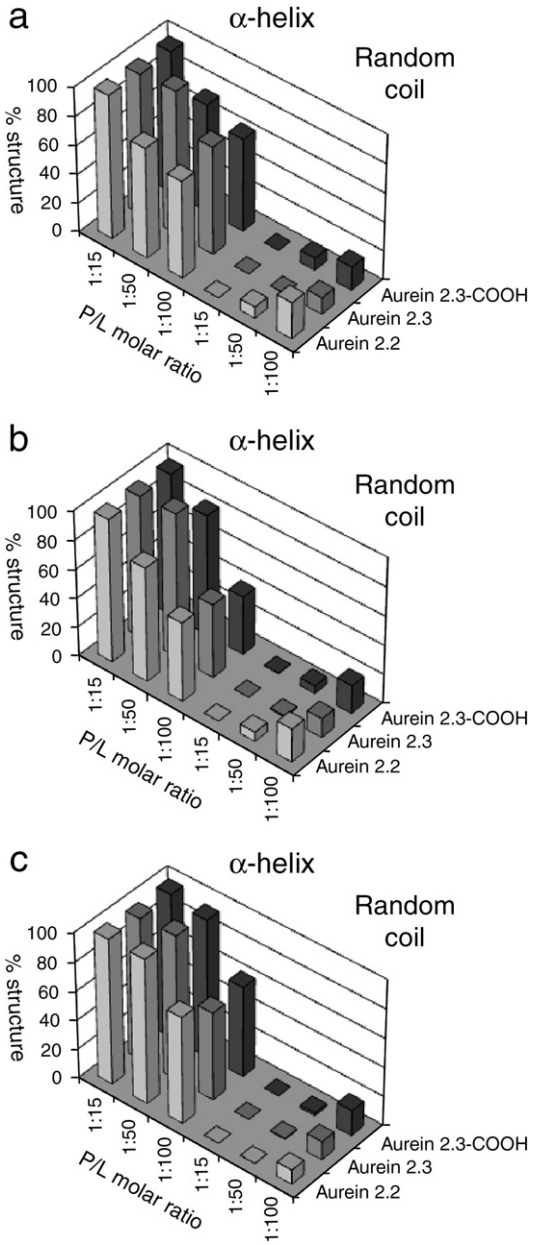

Fig. 1. Secondary structural content of aurein 2.2, aurein 2.3, and aurein 2.3-COOH in 1:1 POPC/POPG (mol/mol), 1:1 CL/POPG (mol/mol), and 1:1 POPE/POPG (mol/mol) SUVs: percentage α-helical and random coil content were plotted as a function of P/L molar ratios and peptides in the presence of (a) 1:1 POPC/POPG (mol/mol), (b) 1:1 CL/POPG (mol/mol), and (c) 1:1 POPE/POPG (mol/mol) SUVs. The plots show that for all membrane compositions, the percentage of α-helical content decreased and the percentage of random coil content increased as the P/L ratio decreased.

following section), samples were prepared in similar fashion so that the data sets could be compared directly and also to verify that the samples were aligned. All experiments were conducted at 30 °C (liquid crystalline phase) for consistent comparison with our previous studies. In addition, experiments were repeated at least twice to ensure the reproducibility of the results.

Fig. 3 shows the OCD results for aurein 2.2, aurein 2.3, and aurein 2.3-COOH in 1:1 CL/POPG (mol/mol) and 1:1 POPE/POPG (mol/mol) bilayers as a function of P/L ratios. The spectra were normalized such that all intensities at 222 nm had the same value. The spectra show that these three peptides had similar insertion profiles in CL/POPG bilayers as in 1:1 POPC/POPG (mol/mol) bilayers [22] but had dramatically different insertion profiles in POPE/POPG bilayers. In the presence of POPE/POPG, both aurein 2.2 and aurein 2.3 showed a

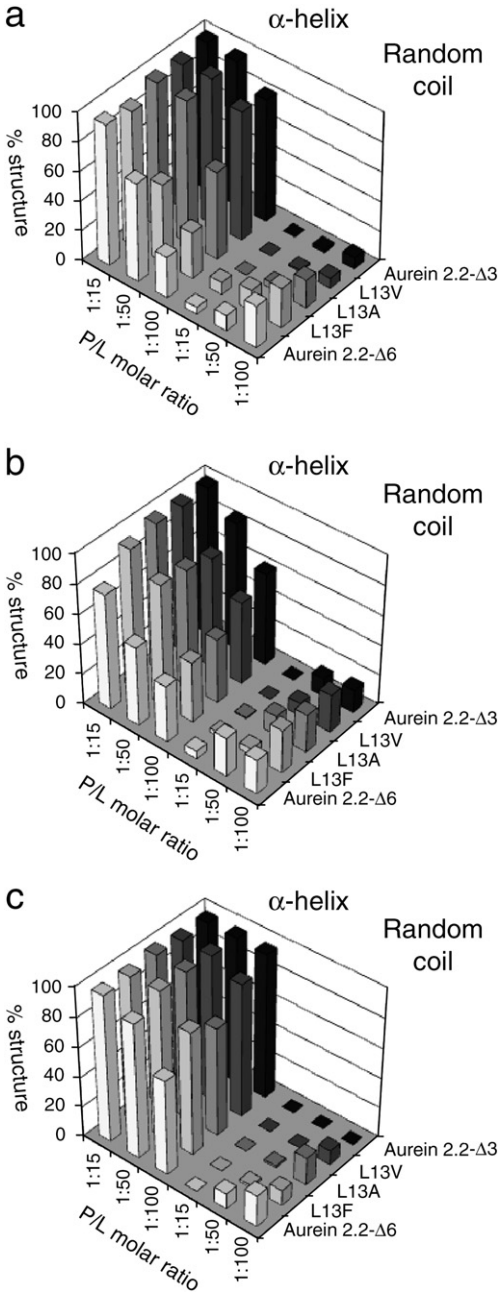

Fig. 2. Secondary structural content of the five aurein variants in 1:1 POPC/POPG (mol/mol), 1:1 CL/POPG (mol/mol), and 1:1 POPE/POPG (mol/mol) SUVs: percentage α-helical and random coil content were plotted as a function of P/L molar ratios and peptides in the presence of (a) 1:1 POPC/POPG (mol/mol); (b) 1:1 CL/POPG (mol/mol); and (c) 1:1 POPE/POPG (mol/mol) SUVs. The plots show that for all membrane compositions, the percentage of α-helical content decreased and the percentage of random coil content increased as the P/L ratio decreased.

very gradual insertion profile over all P/L ratios, with a high proportion of the signal being characteristic of that observed for the surface adsorbed state (S-state). The peptide aurein 2.3-COOH remained fully in the S-state over the concentration ranges probed here. This indicates that aurein 2.2, aurein 2.3, and aurein 2.3-COOH behaved similarly in POPC/POPG and CL/POPG bilayers, but not in POPE/POPG bilayers.

Fig. 4 shows the OCD results for the five aurein variants in 1:1 POPE/POPG (mol/mol) bilayers as a function of P/L ratios. The spectra showed that L13A, L13F, and aurein 2.2-Δ6 inserted into POPE/POPG bilayers at threshold P/L molar ratios between 1:15 and 1:80, and become surface adsorbed at P/L ratios greater than 1:80. Aurein 2.2-Δ3 and L13V did not insert at all P/L ratios examined. This is in stark contrast to what was previously observed in 1:1 POPC/POPG (mol/mol) bilayers, where L13V, L13F, and aurein 2.2-Δ3 inserted at low peptide concentrations, which is consistent with the ability of these peptides to kill *S. aureus* via membrane perturbation (cf. [23]). Aurein 2.2-Δ6, on the other hand, had a similar insertion profile as previously observed in POPC/POPG bilayers. Generally all aurein variants inserted less readily into POPE/POPG membranes than into POPC/POPG membranes, with the exception of aurein 2.2-Δ6. Overall, these data illustrate that the choice of the different model bacterial membranes had a significant impact on the observed aurein peptide insertion profiles.

3.3. Lipid headgroup perturbation by the aurein peptides

^{31}P NMR spectra were recorded for aurein 2.2, aurein 2.3, and aurein 2.3-COOH in 1:1 CL/POPG (mol/mol) and 1:1 POPE/POPG (mol/mol) bilayers (Figs. 5 and 6). The ^{31}P NMR experiments were conducted to determine whether the insertion of the peptides was accompanied by a perturbation of the lipid headgroups and whether this membrane disruption occurred via a barrel-stave model, carpet model, or toroidal pore model [51–55]; a micellar aggregate channel model [56,57]; or a detergent-like mechanism [21].

In the absence of aurein 2.2, aurein 2.3, or aurein 2.3-COOH, the spectra of 1:1 CL/POPG (mol/mol) bilayers consisted of a single peak at ~8.7 ppm, which indicated that the lipid bilayers were aligned with their normal parallel to the magnetic field and that the headgroups were somewhat mobile due to the scaled shift (Fig. 5). ^{31}P NMR spectra of CL/POPG multilamellar vesicles consisted of a line at 8.7 ppm superimposed on a powder pattern spanning the range of -10 to 30 ppm, reminiscent of the spectra seen in Fig. 5d. Spectra of aligned CL or POPG alone consisted of a single sharp line at 8.7 ppm. This suggests that our preparation of aligned samples containing CL and/or POPG yields aligned hydrated films where a certain degree of headgroup mobility is maintained. In the presence of the three peptides, the spectra showed slightly increased powder pattern signal in the -10 to 30 ppm range, indicative that the peptides perturb the lipid alignment. The proportion of the powder pattern signal increased as the peptide concentration increased (see figure caption for proportion of unaligned signal [10,58]). This indicates that the membrane disordering was concentration-dependent. At high peptide concentrations, all aurein parents showed a relatively similar extent of disordering. At low peptide concentrations, aurein 2.2 exhibited a more disruptive effect than aurein 2.3 and aurein 2.3-COOH. In the presence of aurein 2.3-COOH at low concentrations, only slightly broadened peaks were observed. This suggests that aurein 2.3-COOH did not have a significant disordering effect on CL/POPG bilayers, which is consistent with our previous ^{31}P NMR results in 4:1 POPC/POPG bilayers [22].

In the absence of aurein 2.2, aurein 2.3 or aurein 2.3-COOH, the spectra of POPE/POPG bilayers consisted primarily of two single resonances at 30 ppm (PE) and 15 ppm (PG), which indicated that the lipid bilayers were aligned with their normal parallel to the magnetic field (Fig. 6). In the presence of each of the three peptides, however, the spectra showed slightly broadened peaks at 30 ppm, indicating increased contribution from unaligned ^{31}P headgroups. In addition, a powder pattern signal was also observed in the -10 to 30 ppm range, indicative of random headgroup orientations (see figure caption for proportion of unaligned signal [10,58]) (Fig. 6). The membrane disordering effect was again found to be concentration-dependent and peptide-specific. At high peptide concentrations, the spectra consisted mostly of signal arising from a powder pattern, and the effect was more prominent for aurein 2.2 than the other two peptides. If one were to correlate the trends observed here to activity, then one would expect that aurein 2.2 was more effective at killing Gram

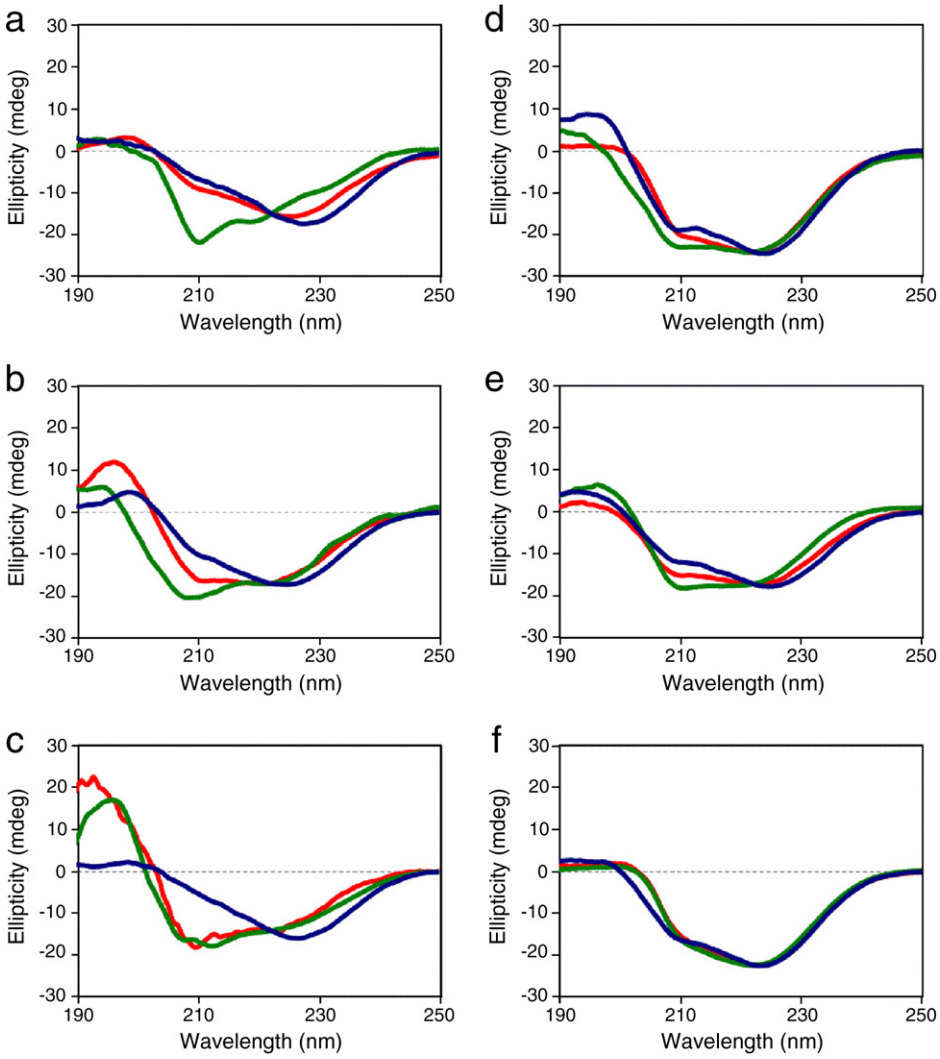

Fig. 3. Oriented CD spectra of aurein 2.2, aurein 2.3, and aurein 2.3-COOH in 1:1 CL/POPG (mol/mol) (left panels) and 1:1 POPE/POPG (mol/mol) (right panels) bilayers: (a and d) aurein 2.2; (b and e) aurein 2.3; and (c and f) aurein 2.3-COOH (P/L molar ratios = 1:15 (blue), 1:80 (red), and 1:120 (green)). The spectra were normalized such that intensities of all spectra at 222 nm are the same. The spectra show that the insertions of these three aurein peptides into 1:1 CL/POPG (mol/mol) bilayers in similar as in 1:1 POPC/POPG (mol/mol) bilayers [22]. In the presence of 1:1 POPE/POPG (mol/mol) bilayers, these aurein peptides retain a lot of the S-state characteristics at all the P/L ratios tested here.

positive bacteria such as *B. cereus* than aurein 2.3 or aurein 2.3-COOH, which are equally effective.

When the five different aurein variants were added to 1:1 POPE/POPG (mol/mol) bilayers, different effects on the bilayer headgroups were observed. When the L13 variants (i.e. L13A, L13V, and L13F) were added at high concentrations, the spectra showed an increased contribution from an underlying powder pattern (see figure caption for proportion of unaligned signal [10,58]) (Fig. 7). At low peptide concentrations, the sizes of the powder pattern were relatively similar. Note that in the presence of the L13V mutant at high concentrations, the powder pattern increased significantly. This suggests that at this concentration, the L13V mutant may be more disruptive to the bilayer headgroup alignment than the other variants, an observation also made for L13V in 4:1 POPC/POPG (mol/mol) bilayers. When the C-terminally truncated variants were added at high concentrations, the spectra again showed enlarged underlying powder pattern (see figure caption for proportion of unaligned signal [10,58]) (Fig. 8). At low peptide concentrations, the sizes of the powder pattern decreased as the aurein 2.2-Δ3 concentration decreased, but stayed relatively constant for aurein 2.2-Δ6. Overall, the trends observed for the mutant peptides in POPE/POPG are reminiscent of those seen in POPC/POPG bilayers. This suggests perhaps that membrane perturbation was mainly driven by electrostatic interactions between the positively charged peptides and the negatively charged PG headgroups, and was less dependent on the composition of the partner lipid, i.e. be it PC or PE [59].

Taken together, the presence of powder patterns in the ^{31}P NMR data suggests that all aurein peptides disorder the bilayer headgroups by forming toroidal pores or disordered pores as found in the aggregate model [51–55], be that in POPC/POPG, CL/POPG, or POPE/POPG membranes. The extent of the membrane perturbation was found to be strongly concentration-dependent and partly dependent on the nature of the peptide.

3.4. Antimicrobial activity of the aurein peptides

MICs of the aurein 2.2, aurein 2.3, aurein 2.3-COOH and the five additional aurein peptides against *B. cereus*, *P. aeruginosa*, and *E.coli* were determined. The MICs, reported in Table 1, indicated that all the aurein peptides had very low to no activities against these bacterial strains, in contrast to our observations in *S. aureus* [43]. The MICs determined for both aurein 2.2 and 2.3 against *B. cereus* were consistent with previously reported literature values [60]. The MIC results suggest that the aurein peptides are ineffective against bacteria

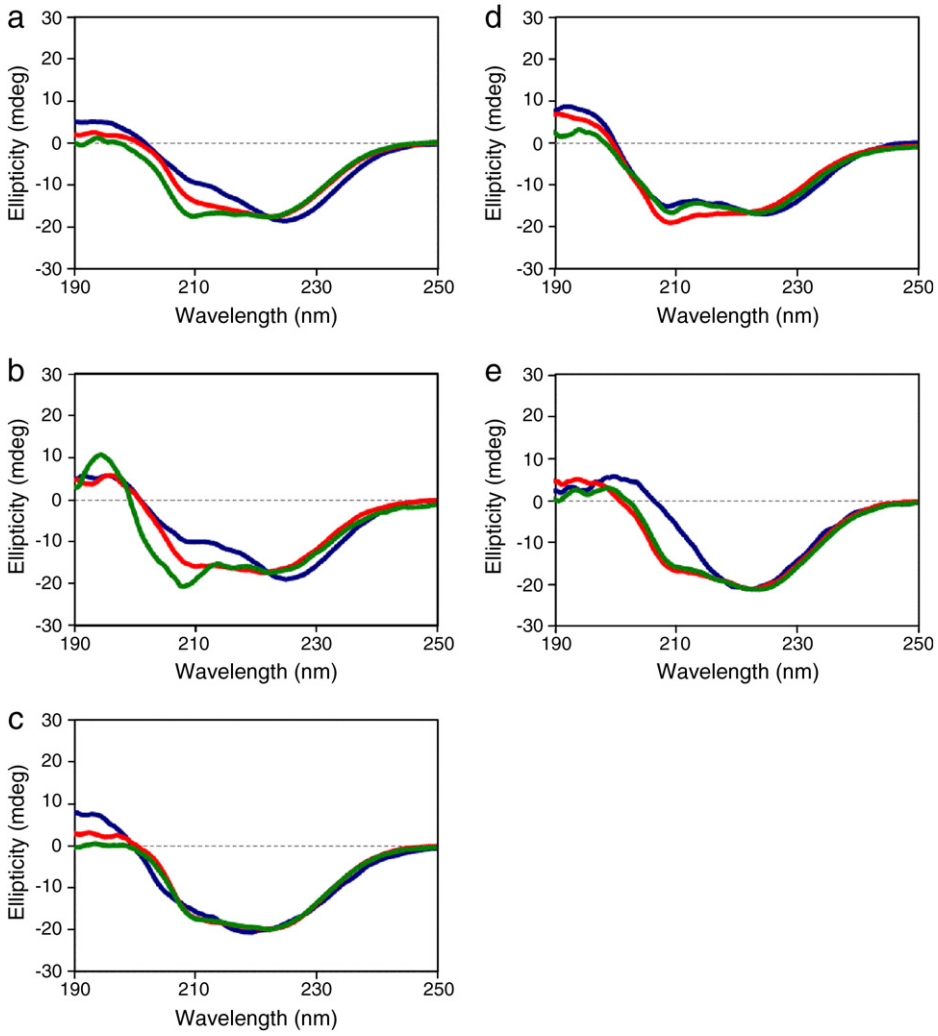

Fig. 4. Oriented CD spectra of the five aurein variants in 1:1 POPE/POPG (mol/mol) bilayers: (a) L13A, (b) L13F, (c) L13V, (d) aurein 2.2-Δ3, and (e) aurein 2.2-Δ6 (P/L molar ratios = 1:15 (blue), 1:80 (red), and 1:120 (green)). The spectra were normalized such that intensities of all spectra at 222 nm are the same. The spectra show that the aurein variants inserted into 1:1 POPE/POPG (mol/mol) bilayers at threshold P/L molar ratios between 1:15 and 1:80 for L13A, L13F and aurein 2.2-Δ6, and remained in the S-state for L13V and aurein 2.2-Δ3. These results were significantly different from those obtained in 1:1 POPC/POPG (mol/mol) bilayers.

with high PE content in their membranes. In addition, the MIC results correlated with the oriented CD and ^{31}P NMR results obtained in POPE/POPG model membranes.

4. Discussion

A critical step in unlocking the mechanism of action of a given antimicrobial peptide is to understand how membrane composition modulates structure and peptide–lipid interactions. In this contribution, we have further investigated how two antimicrobial peptides from the Australian Southern Bell frog *Litoria aurea*, namely aurein 2.2 and aurein 2.3, and some of their variants interact with a range of currently used model bacterial membranes. We have also examined the peptide–lipid interaction of the inactive analogue aurein 2.3-COOH.

Bacterial membrane composition varies from bacteria to bacteria and also as a response to changing environment [61,62] and to exposure to antibiotics [63–65]. It is well known that different bacterial strains can have unique membrane compositions [27,65–70]. For example, Gram positive bacteria have a membrane composition that is different from their Gram negative counterparts [42]. Even among the Gram positive bacteria themselves, different membrane compositions have been identified. Both *S. aureus* and *S. pneumonia* have ~50:50 CL/PG (% of total lipids), whereas *B. cereus* and *B. anthracis* have ~43:40 PE/PG (% of total lipids). A slightly higher percentage of PE in the total membrane lipids was found for *B. polymyxa* (~60%), whereas as high as 70% PG was detected from *B. subtilis*. For Gram negative bacteria, *E. coli*, *E. cloacae*, *P. mirabilis*, and *K. pneumonia* have ~80% PE, whereas *Y. kristensenii* and *P. aeruginosa* have ~60% PE (with PG being the next highest constituent). Most Gram negative bacteria have a relatively low percentage of CL.

Since *S. aureus* is the main antimicrobial target for the aurein peptides, incorporating CL and PG into model membranes is necessary to replicate biologically relevant membranes. Alternatively, a 1:1 mixture of PE/PG may be another ideal model membrane, in particular to mimic bacteria such as *B. cereus* and *B. anthracis*. Choosing the correct source of the lipids (i.e. natural versus synthetic) is important. In order to have a well defined membrane, synthetic lipids are often selected since these lipids can be obtained in pure form. Thus the POPC, POPG and POPE used in this study were synthetic. For CL, the only readily available synthetic forms are tetramyristoylcardiolipin (TMCL), tetrapalmitoylcardiolipin (TPCL), and tetraoleoylcardiolipin (TOCL). The high T_m of TMCL (~47 °C), TPCL (~62 °C) [71], and *E. coli* cardiolipins [72] would require experiments to be conducted at the high temperatures needed to achieve the liquid crystalline phase and make comparison of data obtained at 30 °C for POPC/POPG or POPE/

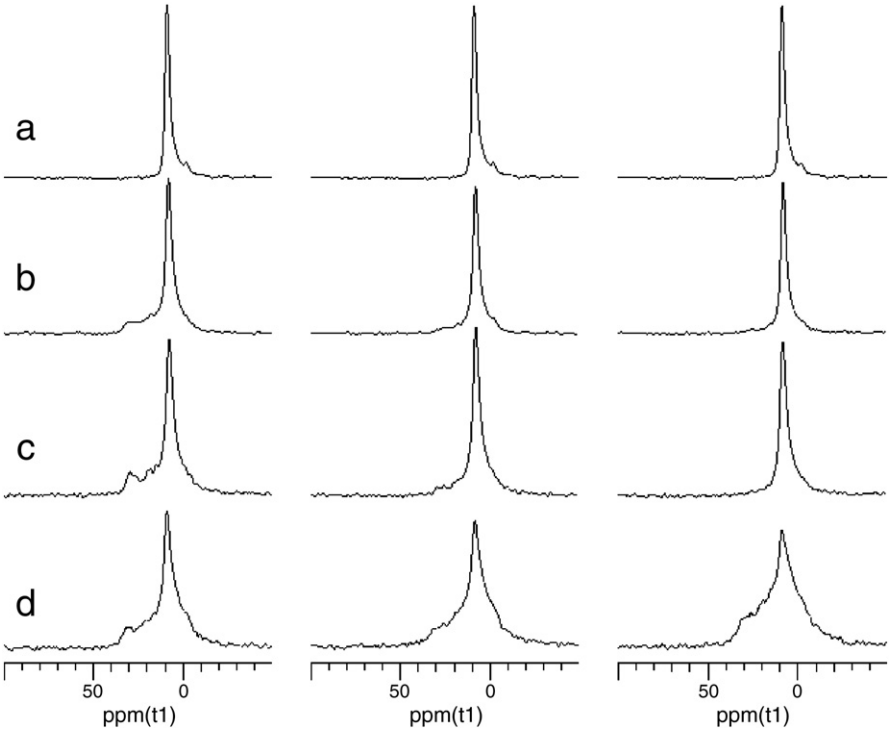

Fig. 5. Solid state ^{31}P NMR spectra of mechanically aligned 1:1 CL/POPG (mol/mol) bilayers containing aurein 2.2, aurein 2.3, and aurein 2.3-COOH: (a) CL/POPG bilayers alone, P/L = (b) 1:120, (c) 1:80, and (d) 1:15 in the presence of aurein 2.2 (left panel), aurein 2.3 (centre panel), and aurein 2.3-COOH (right panel). The spectra were recorded using 2048 scans at 30°C, oriented such that the normal bilayer was parallel to the external magnetic field. The spectra were processed with 50 Hz line-broadening. At P/L ratios of 1:15, the proportion of unaligned lipids increases by 63% for aurein 2.2, 63% for aurein 2.3, and 71% for aurein 2.3-COOH. These percentages are determined by fitting the spectra using 1 Gaussian/Lorentzian lines and 1 ^{31}P CSA static line in DMFIT [84] and integrating.

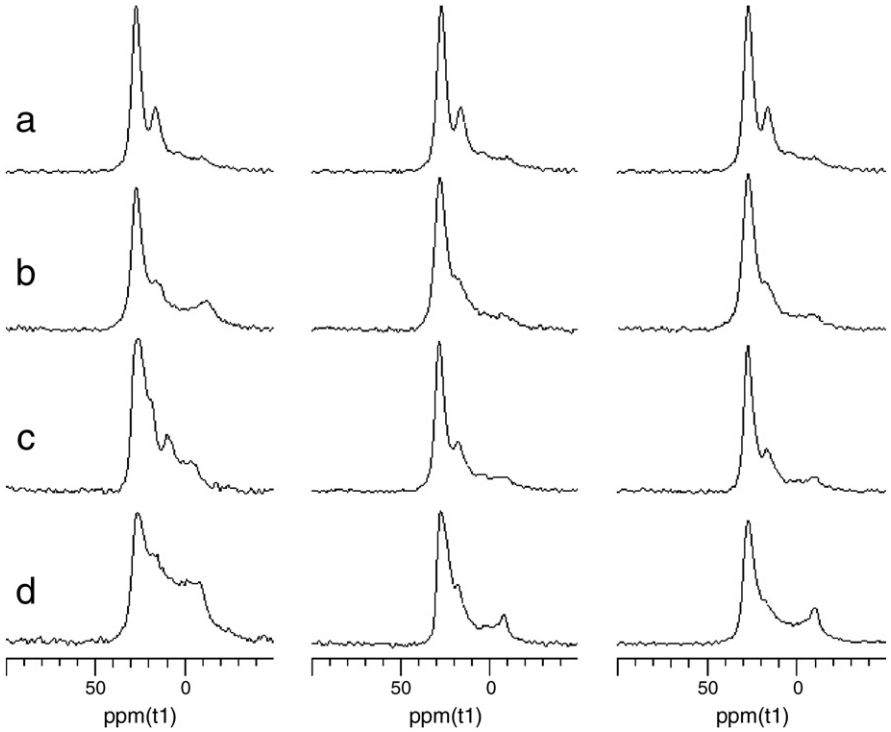

Fig. 6. Solid state ^{31}P NMR spectra of mechanically aligned 1:1 POPE/POPG (mol/mol) bilayers containing aurein 2.2, aurein 2.3, and aurein 2.3-COOH: (a) POPE/POPG bilayers alone, P/L = (b) 1:120, (c) 1:80, and (d) 1:15 in the presence of aurein 2.2 (left panel), aurein 2.3 (centre panel), and aurein 2.3-COOH (right panel). The spectra were recorded using 2048 scans at 30°C, oriented such that the normal bilayer was parallel to the external magnetic field. The spectra were processed with 50 Hz line-broadening. At P/L ratios of 1:15, the proportion of unaligned lipids increases by 40% for aurein 2.2, 15% for aurein 2.3, and 24% for aurein 2.3-COOH. These percentages are determined by fitting the spectra using 2 Gaussian/Lorentzian lines and 1 ^{31}P CSA static line in DMFIT [84] and integrating.

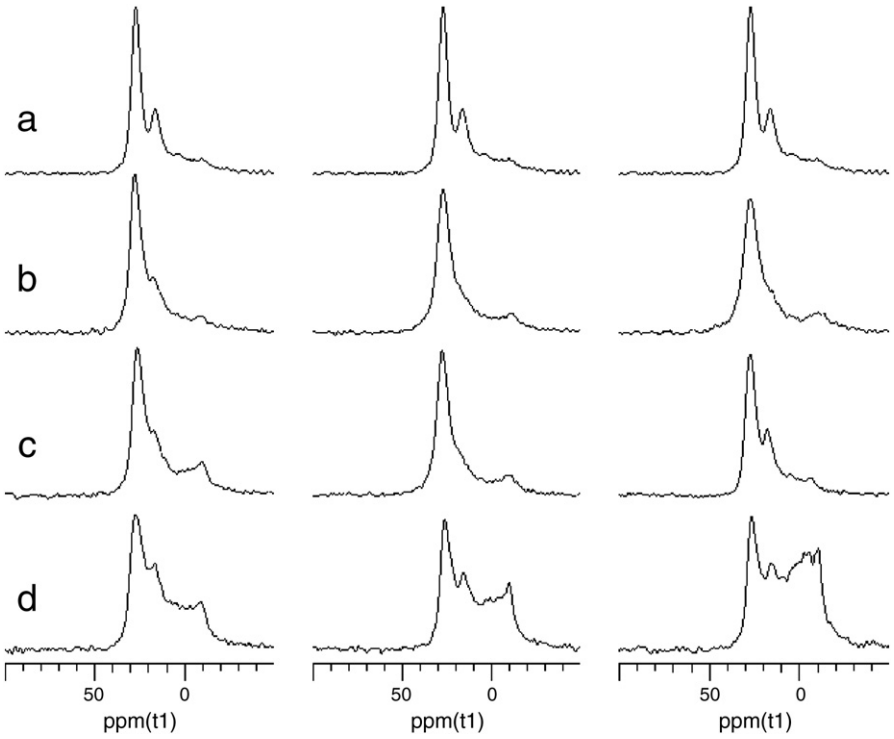

Fig. 7. Solid state ^{31}P NMR spectra of mechanically aligned 1:1 POPE/POPG (mol/mol) bilayers containing the three L13 aurein variants: (a) POPE/POPG bilayers alone, P/L = (b) 1:120, (c) 1:80, and (d) 1:15 in the presence of L13A (left panel), L13F (centre panel), and L13V (right panel). The spectra were recorded using 2048 scans at 30 °C, oriented such that the normal bilayer was parallel to the external magnetic field. The spectra were processed with 50 Hz line-broadening. At P/L ratios of 1:15, the proportion of unaligned lipids increases by 30% for L13A, 40% for L13F, and 59% for L13V. These percentages are determined by fitting the spectra using 2 Gaussian/Lorentzian lines and 1 ^{31}P CSA static line in DMFIT [84] and integrating.

POPG with data obtained at higher temperatures for CL/POPG difficult. TOCL or bovine heart CL are more attractive alternatives, with a T_m below 0°C [73]. In this study, we therefore chose to use a bovine heart CL:POPG mixture as a model membranes for *S. aureus* [74]. A control CD experiment using aurein 2.2 in 1:1 TOCL/POPG (mol/mol) (data not shown) yielded the same results as those obtained for 1:1 bovine heart CL/POPG shown in Fig. 1b.

It is widely accepted that most cationic antimicrobial peptides adopt defined secondary structures only in the presence of membranes [51,75,76], and that the adoption of secondary structure is a key first step during membrane interaction. Our solution CD results demonstrated that the eight aurein peptides tested here maintain their predominantly α-helical structure in 1:1 CL/POPG (mol/mol) and 1:1 POPE/POPG (mol/mol) as well as in 1:1 POPC/POPG [22] SUVs. This is particularly true for P/L ratios of 1:50 or higher. Very few studies have demonstrated that amphibian antimicrobial peptides preserve their predominant conformation in both POPC/POPG and POPE/POPG membranes. To the best of our knowledge, only one molecular dynamics (MD) simulation and lipid vesicle study has shown that buforin II (BF2), an α–helical antimicrobial peptide from the asian toad *Bufo bufo gargarizans*, maintains its predominant structure in both POPC/POPG and POPE/POPG membranes [77]. The presence of PE does not alter secondary structure, nor does it abolish the ability of a peptide to bind to the lipid membranes. A recent review of protegrin-1 (PG-1) demonstrated analogous observations in that PG-1 preserves its β-sheet structure in POPC/Chol bilayers as well as in POPE/POPG bilayers [9]. The solution CD data on the aurein peptides has demonstrated that the choice of PC versus CL versus PE in bacterial model membranes has consequences only for the structural content, but not for the overall structure of the peptide. Indeed, at low peptide concentrations, the aurein peptides generally were less helical in CL/PG, followed by PC/PG, and finally, PE/PG (Figs. 1 and 2; P/L = 1:100). The study of BF2 also demonstrated that the presence of PE induced a higher percentage of helical content in BF2 than PC [77]. The higher percentage of helicity, however, does not necessarily correlate with higher antimicrobial activity or greater ability to disorder membranes. Indeed, a recent study of four α-helical antimicrobial peptides indicated that flexibility in the structure can actually promote better peptide association into toroidal pores and thus better toroidal pore formation [78]. Overall, the structural findings suggest that the presence of secondary structure cannot necessarily be used as an indicator of how well a given antimicrobial peptide will interact with different lipids.

Cationic antimicrobial peptides interact with bacterial membranes mainly through electrostatic interactions with the PG headgroups [28,52]. If, however, the interaction with the PG headgroups were the only governing factor, then one would expect that the exact nature of additional lipid components would be irrelevant. The OCD data presented here suggests that the choice of PC versus CL versus PE plays a significant role in the ability of the aurein peptides to insert. Indeed, aurein 2.2, aurein 2.3, and aurein 2.3-COOH inserted much less readily into POPE/POPG bilayers, than POPC/POPG or CL/POPG membranes, which were roughly equivalent. Our OCD results on all five aurein variants further support this finding. Studies have suggested that PE/PG bilayers have stronger headgroup–headgroup interactions than PC/PG (and presumably also CL/PG), because the shapes of PE and PG are more complementary. Tighter lipid packing will of course impede peptide insertion [59]. The choice of PC versus CL versus PE appears to play less of a role however in how the aurein peptides perturb the lipid headgroups. The ^{31}P NMR data suggested that all aurein peptides disordered the bilayer headgroups by forming of interactions reminiscent of distorted toroidal pores [51–55], be that in POPC/POPG, CL/POPG, or POPE/POPG membranes. The extent of membrane perturbation is only found to be strongly concentration-dependent and partially dependent on the nature of the peptide. In the literature, several quite diverse antimicrobial peptides perturb

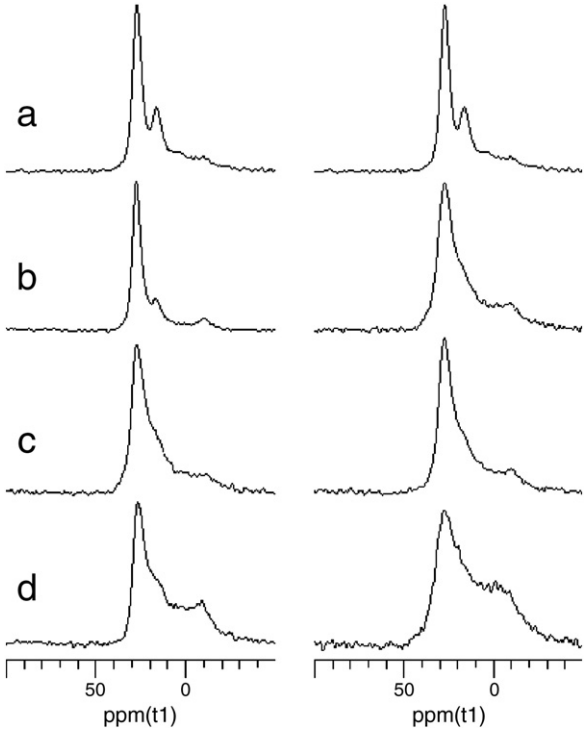

Fig. 8. Solid state ^{31}P NMR spectra of mechanically aligned 1:1 POPE/POPG (mol/mol) bilayers containing the two C-terminally truncated aurein variants: (a) POPE/POPG bilayers alone, P/L = (b) 1:120, (c) 1:80, and (d) 1:15 in the presence of aurein 2.2-Δ3 (left panel) and aurein 2.2-Δ6 (right panel). The spectra were recorded using 2048 scans at 30 °C, oriented such that the normal bilayer was parallel to the external magnetic field. The spectra were processed with 50 Hz line-broadening. At P/L ratios of 1:15, the proportion of unaligned lipids increases by 31% for aurein 2.2-Δ3 and 40% for aurein 2.2-Δ6. These percentages are determined by fitting the spectra using 2 Gaussian/Lorentzian lines and 1 ^{31}P CSA static line in DMFIT [84] and integrating.

membranes similarly [51,53,55,79,80], be that in POPC, POPC/POPG, POPE, and POPE/POPG bilayers. Examples include MSI-78 [27,81,82], KIGAKI [83], and PG-1 [8–10].

As the MIC data show, the aurein peptides were not very active against bacteria that contain ~40–60% PE, namely bacteria like *B. cereus* and *P. aeruginosa*. The biophysical data correlated with this low activity since for 1:1 POPE/POPG, all the aurein peptides are found to insert into PE/PG membranes to a lesser extent than PC/PG. The high helicity found in POPE/POPG suggests that secondary structure per se cannot be used as an indicator of activity. For completeness, the MIC of each aurein peptide was determined for *E.coli* (80% PE), as well as the effect of the peptides on 4:1 POPE/POPG headgroups using ^{31}P NMR on aligned bilayers (Figs. S4 and S5). Interestingly, the data suggested that certain of the aurein peptides had some minimal level of activity, yet did not perturb the lipid headgroups as well as when the peptides were in 1:1 POPE/POPG. Therefore, in this case, one would have to conclude that a membrane model of 4:1 POPE/POPG (or even 1:1 POPE/POPG) would be inadequate for determining the mode of action of the aurein peptides that showed some minimal activity against *E. coli*. In addition, the minimal perturbation seen in 4:1 POPE/POPG model membranes and the residual activity observed might suggest that the aurein peptides may affect *E. coli* by acting on some internal target, rather than perturbing the membrane directly. Nevertheless, the MIC data determined previously against *S. aureus* [43] showed that the aurein peptides are quite effective at killing these bacteria and that 1:1 POPC/POPG or 1:1 CL/POPG bilayers are a good choice as model membranes for this bacteria.

Understanding the behavior of a given amphibian antimicrobial peptide in both intact bacteria and model membranes can reveal what is the basis for activity against certain bacteria and is important in any future design of better antimicrobial agents. For the aurein peptides, a good model for understanding how these peptides act on *S. aureus* is 1:1 POPC/POPG or 1:1 CL/POPG. For *B. cereus*, model membranes of 1:1 POPE/POPG are a good choice. In conclusion, specific model membranes should be used to model specific bacteria, given the unique membrane composition of individual bacterial species.

Acknowledgements

The authors thank Fred Rossell of the Laboratory of Molecular Biophysics Spectroscopy hub for his help in maintaining the CD, infrastructure obtained via CFI funding. R.E.W.H. acknowledges funding from the Advanced Food and Materials Network and the Canadian Institutes for Health Research. J.D.H. received a Canadian Commonwealth Post-Doctoral Research Fellowship. S.K.S. gratefully acknowledges the support of the National Sciences and Engineering Research Council of Canada through a Discovery Grant, and the Michael Smith Foundation for Health Research through a Career Investigator Award. R.E.W.H. is the recipient of a Canada Research Chair.

Appendix A. Supplementary data

Supplementary data to this article can be found online at doi:10.1016/j.bbamem.2010.11.025.

References

[1] R.E. Hancock, H.G. Sahl, Antimicrobial and host-defense peptides as new anti-infective therapeutic strategies, Nat. Biotechnol. 24 (2006) 1551–1557.
[2] I. Marcotte, K.L. Wegener, Y.H. Lam, B.C. Chia, M.R. de Planque, J.H. Bowie, M. Auger, F. Separovic, Interaction of antimicrobial peptides from Australian amphibians with lipid membranes, Chem. Phys. Lipids 122 (2003) 107–120.
[3] F. Porcelli, B.A. Buck-Koehntop, S. Thennarasu, A. Ramamoorthy, G. Veglia, Structures of the dimeric and monomeric variants of magainin antimicrobial peptides (MSI-78 and MSI-594) in micelles and bilayers, determined by NMR spectroscopy, Biochemistry 45 (2006) 5793–5799.
[4] Y. Wu, K. He, S.J. Ludtke, H.W. Huang, X-ray diffraction study of lipid bilayer membranes interacting with amphiphilic helical peptides: diphytanoyl phosphatidylcholine with alamethicin at low concentrations, Biophys. J. 68 (1995) 2361–2369.
[5] P.C. Dave, E. Billington, Y.L. Pan, S.K. Straus, Interaction of alamethicin with ether-linked phospholipid bilayers: oriented circular dichroism, 31P solid-state NMR, and differential scanning calorimetry studies, Biophys. J. 89 (2005) 2434–2442.
[6] U. Harzer, B. Bechinger, Alignment of lysine-anchored membrane peptides under conditions of hydrophobic mismatch: a CD, 15 N and 31P solid-state NMR spectroscopy investigation, Biochemistry 39 (2000) 13106–13114.
[7] P. Tremouilhac, E. Strandberg, P. Wadhwani, A.S. Ulrich, Synergistic transmembrane alignment of the antimicrobial heterodimer PGLa/magainin 2, J. Biol. Chem. 281 (2006) 32089–32094.
[8] R. Mani, S.D. Cady, M. Tang, A.J. Waring, R.I. Lehrer, M. Hong, Membrane-dependent oligomeric structure and pore formation of a beta-hairpin antimicrobial peptide in lipid bilayers from solid-state NMR, Proc. Natl Acad. Sci. USA 103 (2006) 16242–16247.
[9] T. Chen, C. Scott, L. Tang, M. Zhou, C. Shaw, The structural organization of aurein precursor cDNAs from the skin secretion of the Australian green and golden bell frog, Litoria aurea, Regul. Pept. 128 (2005) 75–83.
[10] S. Wi, C. Kim, Pore structure, thinning effect, and lateral diffusive dynamics of oriented lipid membranes interacting with antimicrobial peptide protegrin-1: 31P and 2 H solid-state NMR study, J. Phys. Chem. B 112 (2008) 11402–11414.
[11] J.A. Patch, A.E. Barron, Helical peptoid mimics of magainin-2 amide, J. Am. Chem. Soc. 125 (2003) 12092–12093.
[12] L. Picas, A. Carretero-Genevrier, M.T. Montero, J.L. Vazquez-Ibar, B. Seantier, P.E. Milhiet, J. Hernandez-Borrell, Preferential insertion of lactose permease in phospholipid domains: AFM observations, Biochim. Biophys. Acta (1798) 1014–1019.
[13] L. Picas, M.T. Montero, A. Morros, J.L. Vazquez-Ibar and J. Hernandez-Borrell, Evidence of phosphatidylethanolamine and phosphatidylglycerol presence at the annular region of lactose permease of Escherichia coli. Biochim. Biophys. Acta, 1798, 291-296.
[14] D. Jung, A. Rozek, M. Okon, R.E.W. Hancock, Structural transitions as determinants of the action of the calcium-dependent antibiotic daptomycin, Chem. Biol. 11 (2004) 949–957.
[15] K. Lohner, E. Staudegger, E.J. Prenner, R.N. Lewis, M. Kriechbaum, G. Degovics, R.N. McElhaney, Effect of staphylococcal delta-lysin on the thermotropic phase behavior and vesicle morphology of dimyristoylphosphatidylcholine lipid bilayer model membranes. Differential scanning calorimetric, 31P nuclear magnetic

resonance and Fourier transform infrared spectroscopic, and X-ray diffraction studies, Biochemistry 38 (1999) 16514–16528.
[16] D. Zweytick, G. Pabst, P.M. Abuja, A. Jilek, S.E. Blondelle, J. Andra, R. Jerala, D. Monreal, G. Martinez de Tejada, K. Lohner, Influence of N-acylation of a peptide derived from human lactoferricin on membrane selectivity, Biochim. Biophys. Acta 1758 (2006) 1426–1435.
[17] S. Thennarasu, D.K. Lee, A. Tan, U. Prasad Kari, A. Ramamoorthy, Antimicrobial activity and membrane selective interactions of a synthetic lipopeptide MSI-843, Biochim. Biophys. Acta 1711 (2005) 49–58.
[18] F.M. Marassi, C. Ma, H. Gratkowski, S.K. Straus, K. Strebel, M. Oblatt-Montal, M. Montal, S.J. Opella, Correlation of the structural and functional domains in the membrane protein Vpu from HIV-1, Proc. Natl Acad. Sci. USA 96 (1999) 14336–14341.
[19] K.J. Hallock, D.K. Lee, J. Omnaas, H.I. Mosberg, A. Ramamoorthy, Membrane composition determines pardaxin's mechanism of lipid bilayer disruption, Biophys. J. 83 (2002) 1004–1013.
[20] T. Doherty, A.J. Waring, M. Hong, Peptide–lipid interactions of the beta-hairpin antimicrobial peptide tachyplesin and its linear derivatives from solid-state NMR, Biochim. Biophys. Acta 1758 (2006) 1285–1291.
[21] B. Bechinger, K. Lohner, Detergent-like actions of linear amphipathic cationic antimicrobial peptides, Biochim. Biophys. Acta 1758 (2006) 1529–1539.
[22] J.T. Cheng, J.D. Hale, M. Elliot, R.E. Hancock, S.K. Straus, Effect of membrane composition on antimicrobial peptides aurein 2.2 and 2.3 from Australian southern bell frogs, Biophys. J. 96 (2009) 552–565.
[23] J.T.J. Cheng, J.D. Hale, J. Kindrachuk, H. Jenssen, M. Elliott, R.E. Hancock, S.K. Straus, Importance of residue 13 and the C-terminus for the structure and activity of the antimicrobial peptide aurein 2.2, Biophys. J. 99 (2010) 2926–2935.
[24] S.M. Gregory, A. Pokorny, P.F. Almeida, Magainin 2 revisited: a test of the quantitative model for the all-or-none permeabilization of phospholipid vesicles, Biophys. J. 96 (2009) 116–131.
[25] S.M. Gupta, C.C. Aranha, J.R. Bellare, K.V. Reddy, Interaction of contraceptive antimicrobial peptide nisin with target cell membranes: implications for use as vaginal microbicide, Contraception 80 (2009) 299–307.
[26] J. Lee, C. Park, S.C. Park, E.R. Woo, Y. Park, K.S. Hahm, D.G. Lee, Cell selectivity-membrane phospholipids relationship of the antimicrobial effects shown by pleurocidin enantiomeric peptides, J. Pept. Sci. 15 (2009) 601–606.
[27] A. Ramamoorthy, S. Thennarasu, D.K. Lee, A. Tan, L. Maloy, Solid-state NMR investigation of the membrane-disrupting mechanism of antimicrobial peptides MSI-78 and MSI-594 derived from magainin 2 and melittin, Biophys. J. 91 (2006) 206–216.
[28] M. Dathe, H. Nikolenko, J. Meyer, M. Beyermann, M. Bienert, Optimization of the antimicrobial activity of magainin peptides by modification of charge, FEBS Lett. 501 (2001) 146–150.
[29] S. Yamaguchi, D. Huster, A. Waring, R.I. Lehrer, W. Kearney, B.F. Tack, M. Hong, Orientation and dynamics of an antimicrobial peptide in the lipid bilayer by solid-state NMR spectroscopy, Biophys. J. 81 (2001) 2203–2214.
[30] J.X. Lu, K. Damodaran, J. Blazyk, G.A. Lorigan, Solid-state nuclear magnetic resonance relaxation studies of the interaction mechanism of antimicrobial peptides with phospholipid bilayer membranes, Biochemistry 44 (2005) 10208–10217.
[31] E.Y. Chekmenev, B.S. Vollmar, K.T. Forseth, M.N. Manion, S.M. Jones, T.J. Wagner, R.M. Endicott, B.P. Kyriss, L.M. Homem, M. Pate, J. He, J. Raines, P.L. Gor'kov, W.W. Brey, D.J. Mitchell, A.J. Auman, M.J. Ellard-Ivey, J. Blazyk, M. Cotten, Investigating molecular recognition and biological function at interfaces using piscidins, antimicrobial peptides from fish, Biochim. Biophys. Acta 1758 (2006) 1359–1372.
[32] K.A. Henzler-Wildman, G.V. Martinez, M.F. Brown, A. Ramamoorthy, Perturbation of the hydrophobic core of lipid bilayers by the human antimicrobial peptide LL-37, Biochemistry 43 (2004) 8459–8469.
[33] C. Leidy, L. Linderoth, T.L. Andresen, O.G. Mouritsen, K. Jorgensen, G.H. Peters, Domain-induced activation of human phospholipase A2 type IIA: local versus global lipid composition, Biophys. J. 90 (2006) 3165–3175.
[34] R.N. Lewis, Y.P. Zhang, R.N. McElhaney, Calorimetric and spectroscopic studies of the phase behavior and organization of lipid bilayer model membranes composed of binary mixtures of dimyristoylphosphatidylcholine and dimyristoylphosphatidylglycerol, Biochim. Biophys. Acta 1668 (2005) 203–214.
[35] A. Mecke, D.K. Lee, A. Ramamoorthy, B.G. Orr, M.M. Banaszak Holl, Membrane thinning due to antimicrobial peptide binding: an atomic force microscopy study of MSI-78 in lipid bilayers, Biophys. J. 89 (2005) 4043–4050.
[36] S.R. Dennison, L.H. Morton, F. Harris, D.A. Phoenix, The impact of membrane lipid composition on antimicrobial function of an alpha-helical peptide, Chem. Phys. Lipids 151 (2008) 92–102.
[37] Y.Q. Xiong, K. Mukhopadhyay, M.R. Yeaman, J. Adler-Moore, A.S. Bayer, Functional interrelationships between cell membrane and cell wall in antimicrobial peptide-mediated killing of Staphylococcus aureus, Antimicrob. Agents Chemother. 49 (2005) 3114–3121.
[38] O. Domenech, G. Francius, P.M. Tulkens, F. Van Bambeke, Y. Dufrene, M.P. Mingeot-Leclercq, Interactions of oritavancin, a new lipoglycopeptide derived from vancomycin, with phospholipid bilayers: Effect on membrane permeability and nanoscale lipid membrane organization, Biochim. Biophys. Acta 1788 (2009) 1832–1840.
[39] V.V. Andrushchenko, M.H. Aarabi, L.T. Nguyen, E.J. Prenner, H.J. Vogel, Thermodynamics of the interactions of tryptophan-rich cathelicidin antimicrobial peptides with model and natural membranes, Biochim. Biophys. Acta 1778 (2008) 1004–1014.
[40] T. Doherty, A.J. Waring, M. Hong, Dynamic structure of disulfide-removed linear analogs of tachyplesin-I in the lipid bilayer from solid-state NMR, Biochemistry 47 (2008) 1105–1116.
[41] R.F. Epand, P.B. Savage, R.M. Epand, Bacterial lipid composition and the antimicrobial efficacy of cationic steroid compounds (Ceragenins), Biochim. Biophys. Acta 1768 (2007) 2500–2509.
[42] R.M. Epand, R.F. Epand, Domains in bacterial membranes and the action of antimicrobial agents, Mol. Biosyst. 5 (2009) 580–587.
[43] Y.L. Pan, J.T.J. Cheng, J.D. Hale, J. Pan, R.E.W. Hancock, S.K. Straus, Characterization of the structure and membrane interaction of the antimicrobial peptides aurein 2.2 and 2.3 from Australian southern bell frogs, Biophys. J. 92 (2007) 2854–2864.
[44] M. Wu, R.E. Hancock, Interaction of the cyclic antimicrobial cationic peptide bactenecin with the outer and cytoplasmic membrane, J. Biol. Chem. 274 (1999) 29–35.
[45] W.C. Johnson, Analyzing protein circular dichroism spectra for accurate secondary structures, Proteins 35 (1999) 307–312.
[46] S.W. Provencher, J. Glockner, Estimation of globular protein secondary structure from circular dichroism, Biochemistry 20 (1981) 33–37.
[47] N. Sreerama, S.Y. Venyaminov, R.W. Woody, Estimation of the number of alpha-helical and beta-strand segments in proteins using circular dichroism spectroscopy, Protein Sci. 8 (1999) 370–380.
[48] N. Sreerama, R.W. Woody, Protein secondary structure from circular dichroism spectroscopy. Combining variable selection principle and cluster analysis with neural network, ridge regression and self-consistent methods, J. Mol. Biol. 242 (1994) 497–507.
[49] N. Sreerama, R.W. Woody, A self-consistent method for the analysis of protein secondary structure from circular dichroism, Anal. Biochem. 209 (1993) 32–44.
[50] N. Sreerama, R.W. Woody, Estimation of protein secondary structure from circular dichroism spectra: comparison of CONTIN, SELCON, and CDSSTR methods with an expanded reference set, Anal. Biochem. 287 (2000) 252–260.
[51] Y. Shai, Mechanism of the binding, insertion and destabilization of phospholipid bilayer membranes by alpha-helical antimicrobial and cell non-selective membrane-lytic peptides, Biochim. Biophys. Acta 1462 (1999) 55–70.
[52] N. Papo, Y. Shai, Host defense peptides as new weapons in cancer treatment, Cell. Mol. Life Sci. 62 (2005) 784–790.
[53] K. Matsuzaki, Why and how are peptide–lipid interactions utilized for self-defense? Magainins and tachyplesins as archetypes, Biochim. Biophys. Acta 1462 (1999) 1–10.
[54] L. Yang, T.M. Weiss, R.I. Lehrer, H.W. Huang, Crystallization of antimicrobial pores in membranes: magainin and protegrin, Biophys. J. 79 (2000) 2002–2009.
[55] H.W. Huang, Action of antimicrobial peptides: two-state model, Biochemistry 39 (2000) 8347–8352.
[56] M. Wu, E. Maier, R. Benz, R.E.W. Hancock, Mechanism of interaction of different classes of cationic antimicrobial peptides with planar bilayers and with the cytoplasmic membrane of Escherichia coli, Biochemistry 38 (1999) 7235–7242.
[57] R.E.W. Hancock, D.S. Chapple, Peptide antibiotics, Antimicrob. Agents Chemother. 43 (1999) 1317–1323.
[58] M. Ouellet, J.D. Doucet, N. Voyer, M. Auger, Membrane topology of a 14-mer model amphipathic peptide: a solid-state NMR spectroscopy study, Biochemistry 46 (2007) 6597–6606.
[59] A. Arouri, M. Dathe, A. Blume, Peptide induced demixing in PG/PE lipid mixtures: a mechanism for the specificity of antimicrobial peptides towards bacterial membranes? Biochim. Biophys. Acta 1788 (2009) 650–659.
[60] T. Rozek, K.L. Wegener, J.H. Bowie, I.N. Olver, J.A. Carver, J.C. Wallace, M.J. Tyler, The antibiotic and anticancer active aurein peptides from the Australian Bell Frogs Litoria aurea and Litoria raniformis the solution structure of aurein 1.2, Eur. J. Biochem. 267 (2000) 5330–5341.
[61] F.E. Frerman, D.C. White, Membrane lipid changes during the formation of a functional electron transport system in *Staphylococcus aureus*, J. Bacteriol. 94 (1967) 1868–1874.
[62] G.H. Joyce, R.K. Hammond, D.C. White, Changes in membrane lipid composition in exponentially growing *Staphylococcus aureus* during the shift from 37 to 25 C, J. Bacteriol. 104 (1970) 323–330.
[63] P.C. Appelbaum, B. Bozdogan, Vancomycin resistance in Staphylococcus aureus, Clin. Lab. Med. 24 (2004) 381–402.
[64] B. Bozdogan, D. Esel, C. Whitener, F.A. Browne, P.C. Appelbaum, Antibacterial susceptibility of a vancomycin-resistant Staphylococcus aureus strain isolated at the Hershey Medical Center, J. Antimicrob. Chemother. 52 (2003) 864–868.
[65] R.S. Conrad, H.E. Gilleland Jr., Lipid alterations in cell envelopes of polymyxin-resistant Pseudomonas aeruginosa isolates, J. Bacteriol. 148 (1981) 487–497.
[66] S. Clejan, T.A. Krulwich, K.R. Mondrus, D. Seto-Young, Membrane lipid composition of obligately and facultatively alkalophilic strains of Bacillus spp, J. Bacteriol. 168 (1986) 334–340.
[67] P.R. Beining, E. Huff, B. Prescott, T.S. Theodore, Characterization of the lipids of mesosomal vesicles and plasma membranes from Staphylococcus aureus, J. Bacteriol. 121 (1975) 137–143.
[68] M.C. Trombe, M.A. Laneelle, G. Laneelle, Lipid composition of aminopterin-resistant and sensitive strains of Streptococcus pneumoniae. Effect of aminopterin inhibition, Biochim. Biophys. Acta 574 (1979) 290–300.
[69] M.A. Haque, N.J. Russell, Strains of Bacillus cereus vary in the phenotypic adaptation of their membrane lipid composition in response to low water activity, reduced temperature and growth in rice starch, Microbiology 150 (2004) 1397–1404.
[70] S. Morein, A. Andersson, L. Rilfors, G. Lindblom, Wild-type Escherichia coli cells regulate the membrane lipid composition in a "window" between gel and non-lamellar structures, J. Biol. Chem. 271 (1996) 6801–6809.
[71] R.N. Lewis, R.N. McElhaney, The physicochemical properties of cardiolipin bilayers and cardiolipin-containing lipid membranes, Biochim. Biophys. Acta 1788 (2009) 2069–2079.

[72] S. Lopes, C.S. Neves, P. Eaton and P. Gameiro, Cardiolipin, a key component to mimic the E. coli bacterial membrane in model systems revealed by dynamic light scattering and steady-state fluorescence anisotropy. Anal. Bioanal. Chem., 398, 1357-66.
[73] R.M. Epand, S. Rotem, A. Mor, B. Berno, R.F. Epand, Bacterial membranes as predictors of antimicrobial potency, J. Am. Chem. Soc. 130 (2008) 14346–14352.
[74] B.D. Fleming, K.M. Keough, Thermotropic mesomorphism in aqueous dispersions of 1-palmitoyl-2-oleoyl- and 1, 2-dilauroyl-phosphatidylglycerols in the presence of excess Na + or Ca2 +, Can. J. Biochem. Cell Biol. 61 (1983) 882–891.
[75] M. Zasloff, Antimicrobial peptides in health and disease, N. Engl. J. Med. 347 (2002) 1199–1200.
[76] R.E.W. Hancock, Cationic peptides: effectors in innate immunity and novel antimicrobials, Lancet Infect. Dis. 1 (2001) 156–164.
[77] E. Fleming, N.P. Maharaj, J.L. Chen, R.B. Nelson, D.E. Elmore, Effect of lipid composition on buforin II structure and membrane entry, Proteins 73 (2008) 480–491.
[78] M. Mihajlovic and T. Lazaridis, Antimicrobial peptides bind more strongly to membrane pores, Biochim. Biophys. Acta.
[79] K. Matsuzaki, Y. Mitani, K.Y. Akada, O. Murase, S. Yoneyama, M. Zasloff, K. Miyajima, Mechanism of synergism between antimicrobial peptides magainin 2 and PGLa, Biochemistry 37 (1998) 15144–15153.
[80] K. Matsuzaki, O. Murase, N. Fujii, K. Miyajima, An antimicrobial peptide, magainin 2, induced rapid flip-flop of phospholipids coupled with pore formation and peptide translocation, Biochemistry 35 (1996) 11361–11368.
[81] K.J. Hallock, D.K. Lee, A. Ramamoorthy, MSI-78, an analogue of the magainin antimicrobial peptides, disrupts lipid bilayer structure via positive curvature strain, Biophys. J. 84 (2003) 3052–3060.
[82] L.M. Gottler, A. Ramamoorthy, Structure, membrane orientation, mechanism, and function of pexiganan–a highly potent antimicrobial peptide designed from magainin, Biochim. Biophys. Acta 1788 (2009) 1680–1686.
[83] J.X. Lu, J. Blazyk, G.A. Lorigan, Exploring membrane selectivity of the antimicrobial peptide KIGAKI using solid-state NMR spectroscopy, Biochim. Biophys. Acta 1758 (2006) 1303–1313.
[84] D. Massiot, F. Fayon, M. Capron, I. King, S. Le Calve, B. Alonso, J.O. Durand, B. Bujoli, Z.H. Gan, G. Hoatson, Modelling one- and two-dimensional solid-state NMR spectra, Magn. Reson. Chem. 40 (2002) 70–76.